JOURNAL OF MATERIALS SCIENCE 27 (1992) 3637–3641

Low-energy ion-beam processing damage in lithium niobate surface-acoustic-wave optical waveguide devices and its post-manufacture removal

C. J. G. KIRKBY
GEC–Marconi Materials Technology Ltd, Caswell, Towcester, Northants., NN12 8EQ, UK

Dry-etch processing of lithium niobate acousto-optic Bragg cells using ion beams of low incident energies (500 eV) induces significant modification to the electrical and electro-mechanical properties of the surface region, severely compromising device operation. The affected properties are largely restored by thermal annealing at relatively low temperatures.

1. Introduction

Monocrystalline lithium niobate is widely utilized as an optical waveguide device substrate on account of its excellent physical properties [1, 2], its strong electro-optic and acousto-optic coefficients rendering it a preferred substrate medium for the fabrication of an expanding repertoire of devices [3]. With the growing application of plasma-based dry-etching procedures in lithium niobate device processing, it is necessary to consider carefully the effects of electron and ion bombardment on substrate properties, particularly those which form the operational basis of the devices under consideration.

Although the majority of studies of lattice modification of lithium niobate by ion bombardment have been performed at relatively high incidence energies, generally sufficient to result in incorporation or implantation, evidence exists for significant lattice modification, particularly in the near-surface region, by lower-energy bombardment. In particular, as will be discussed subsequently, ion bombardment of lithium niobate has been shown to result, not only in the introduction of a measure of surface damage and non-stoichiometry, resulting in an enhanced electrical conductivity, but also of the introduction of significant additional surface acoustic wave attenuation. The appearance of these effects has been confirmed by the present study, which was motivated by the observation that gross variations in acousto-optic efficiency could be correlated with changes in processing conditions during device fabrication [4], optical waveguide functionality remaining unaffected. This observation prompted an examination of the reported effects of low-energy particle bombardment on lithium niobate, the results of which are summarized here.

2. Low-energy bombardment damage in lithium niobate

2.1. Surface crystallography

The influence of ion and electron bombardment on the surface crystallography of lithium niobate has long been of interest on account of the ready modification of surface properties of this material achievable by a variety of agencies. Destefanis *et al.* [5] showed the change in ordinary refractive index consequent on ion bombardment to be a monotonic function of the total energy deposited in nuclear collisions, capable of representation by a single universal curve, valid for all ions. Courths *et al.* [6] observed that Ar^+ bombardment at energies as low as 500 eV resulted in amorphization of the surface, a process anticipated to result in suppression of surface acoustic wave generation. Feng and Shang [7] showed that bombardment of lithium niobate with 600 eV Ar^+ ions resulted in significant departures from stoichiometry in the surface layer, manifested as increases in optical absorption across the entire visible region, together with a large increase in dark conductivity. Both effects disappeared on heating for a few hours at 600 °C, as did the effects reported by Destefanis *et al.* [5]. Klekamp *et al.* [8] demonstrated that electron bombardment induced the desorption of oxygen from lithium niobate at energies as low as 1 keV, the mechanism responsible being identified with the creation of Niobium 4p core-holes followed by an interatomic Auger process leaving oxygen in a highly repulsive state; the time dependence of these processes was subsequently further quantified [9].

2.2. Electrical conductivity

Astakhova *et al.* [10] studied low-temperature argon plasma treatment of lithium niobate, showing that, while no new phases were formed, the sub-surface layer contained interstitial argon ions. In addition, the electrical conductivity was significantly modified, the worst-case resistivity being nearly three orders of magnitude less than that of virgin material and occurring under plasma conditions similar to those employed in fabrication of the devices forming the subject of the

0022–2461

present study. Schreck and Dransfeld [11] reported similar results, showing that relatively low-energy (2 keV) bombardment of lithium niobate with Ar^+ ions resulted in enhancement of electrical conductivity in the region within 5 nm of the surface by up to six orders of magnitude, equivalent to a specific conductivity of $10^3 \Omega$ m at room temperature, with monotonic dependence on bombardment time. The enhanced conductivity was deduced to be non-ionic in origin, since no polarization behaviour was observed. As noted above, Feng and Shang [7] observed unspecified and thermally reversible "large increases in dark conductivity" in the surface region.

2.3. Acoustic attenuation

Hickernell *et al.* [12] demonstrated that piezoelectric coupling efficiency in a proton-exchanged lithium niobate waveguide was considerably reduced as the exchange depth increased towards the acoustic mode depth, suggesting that the resultant lattice modification suppressed the intrinsic piezoelectric properties of the material. Larson *et al.* [13] considered the attenuation of surface acoustic waves in lithium niobate which had been subjected to irradiation by an 80 keV $^{20}Ne^+$ beam at fluences ranging from 10^{18} to 10^{20} ion m^{-2}, showing an acoustic wave attenuation of the form

$$\log[P(z)/P_o] = -Af^n g \quad (1)$$

where P is the acoustic wave power, f is the frequency, z is the distance along the propagation direction and A is a constant for each level of fluence. The constant n is of order 2 for unmodified lithium niobate [14], comparable values being found [13] for the majority of fluence levels investigated. The values determined for the constant A, in units of 10^{-5} dB cm^{-1} MHz^{-2}, ranged from around 0.5 for virgin material, increasing through 1 at a fluence of 10^{18} ion m^{-2} to a maximum of 8 at a fluence of 10^{19} ion m^{-2}; beyond this level, the value declined virtually linearly to 4 at a fluence of 10^{20} ion m^{-2}. Larson *et al.* [13] further suggested that the damage can extend substantially beyond the ion range, noting that disorder extending to a depth a factor of 100 greater than the ion range, even after a 700 °C anneal, had previously been observed in GaAs [15]. No dependence of damage on ion energy was indicated.

2.4. Thermal activation

Common to most of the studies noted above is the observation that the induced damage can generally be reduced, or even eliminated, by thermal annealing. It was shown [11] that the conductivity enhancement following low-energy argon ion bombardment was thermally activated with an energy of 0.41 +/ − 0.04 eV and was further deduced to be non-ionic since no polarization behaviour was observed; on heating to a temperature of the order of 200 °C, a sample previously modified by exposure to argon bombardment was restored to its initial condition. Astakhova *et al.* [10] reported a non-monotonic relationship between conductivity and discharge current, indicating the presence of two competing processes, identified as an activation process, predominating at low current densities, and a rapid etching occurring at high current densities, when the rate of etching predominates over that of surface carrier generation. Tomashpolsky [16] showed that, under vacuum annealing at temperatures in excess of 1300 °C, lithium niobate is significantly less susceptible to thermostimulated surface segregation than other ferroelectric materials.

3. Experimental studies

3.1. Specimens

Acousto-optic devices examined during the course of the present study were designed and fabricated using an established in-house process [4], starting material being 75 mm diameter SAW-grade lithium niobate wafers, procured from the same manufacturer over a period of 3 years. The device structure comprised a sixteen-element beam-steering phased array of interdigital transducers [17], configured for operation at a centre frequency of 1.3 GHz (0.65 μm finger width) and − 3 dB bandwidth of 500 MHz, fabricated by direct-write electron-beam lithography. Following completion of the transducer pattern definition by reactive ion etching with 500 eV argon ions, an initial batch of devices, designated type A in what follows, was subjected to a relatively energetic oxygen plasma-ashing process, with r.f. power of around 500 W, in order to restore surface stoichiometry. These devices were observed to exhibit diffraction efficiencies in the region of 5%, comparable to previous reported behaviour [4]. A subsequent batch of otherwise identical devices, type B, was processed at a much lower, 100 W, power level in order to minimize potential electrode damage; these exhibited complete extinction of the acousto-optic effect, although the optical waveguiding properties at both 633 and 830 nm were unchanged.

3.2. Bombardment simulations

Estimates of the extent of the damage expected to result from ion bombardment during processing were obtained from computer simulation of ion implantation using a procedure based on the PRAL routine described by Zeigler *et al.* [18], utilizing the relevant atomic parameters for argon and lithium niobate. Results for energies in the range 10–50 keV are summarized in Table I, where the "projected range" represents the ionic penetration distance into the substrate, the "straggle" and "lateral spread" quantify the spatial distribution of the implanted ions, and the "electronic range" characterizes the implant range associated with purely electronic stopping. Extrapolation to a processing energy of 500 eV (0.5 keV) indicates a projected range of 1.8 nm, increasing to 60 nm for purely electronic stopping. Fig. 1 shows the anticipated mode profiles of both the optical [19] and acoustic [20] waves, calculated using standard theory. At this energy, the calculated ranges and distributions are significantly less than the depth of either the

TABLE I PRAL simulation of Ar^+ ion implantation in lithium niobate (after Zeigler *et al.* [18])

Energy (keV)	Projected range (μm)	Straggle (μm)	Lateral spread (μm)	Electronic range (μm)
10	0.008	0.004	0.004	0.152
20	0.014	0.006	0.006	0.214
30	0.020	0.008	0.009	0.262
40	0.027	0.011	0.011	0.30
50	0.033	0.013	0.013	0.338

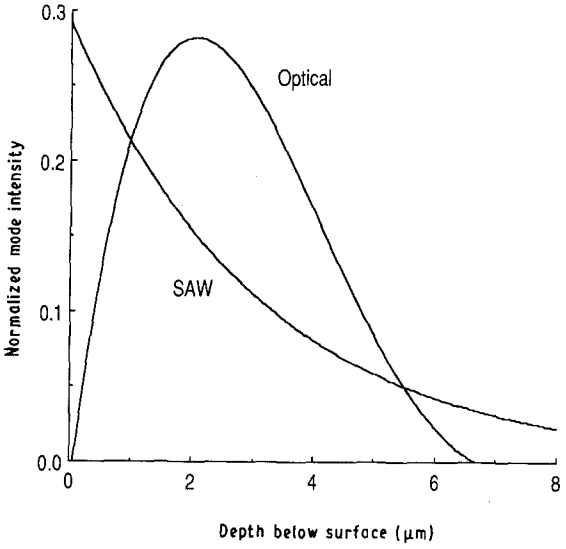

Figure 1 Predicted mode profiles of optical and acoustic waves.

optical or the acoustic mode, suggesting that fundamental implantation mechanisms are not responsible for the drastic modification of characteristics observed here, and confirming the observation of Larson *et al.* [13] that the region of disorder extends substantially beyond the ion range.

3.3. Surface crystallography

In order to identify more precisely the nature of the surface effects existing in the devices under investigation, a systematic analysis of the surface crystallography of lithium niobate was carried out using double-crystal X-ray diffractometry. Using this technique, it is relatively easy to identify the onset of lattice changes, manifesting themselves either as broadening of an intrinsically narrow peak or, in more severe cases, its splitting into two peaks, representing the appearance of two distinct phases. To obtain results rapidly and without disruption to other, ongoing studies, it was necessary to identify a lattice-reflection in Y-cut lithium niobate corresponding to the alignment of the spectrometer current at the time of the measurements; in the circumstances, the $3\,0\,\bar{3}\,0$ lattice reflection, with an inter-plane spacing of $d = 0.1487$ nm, provided a convenient assessment tool.

Fig. 2 shows diffraction results obtained from two samples of virgin material, procured from the same supplier with a time interval of 3 years, the material

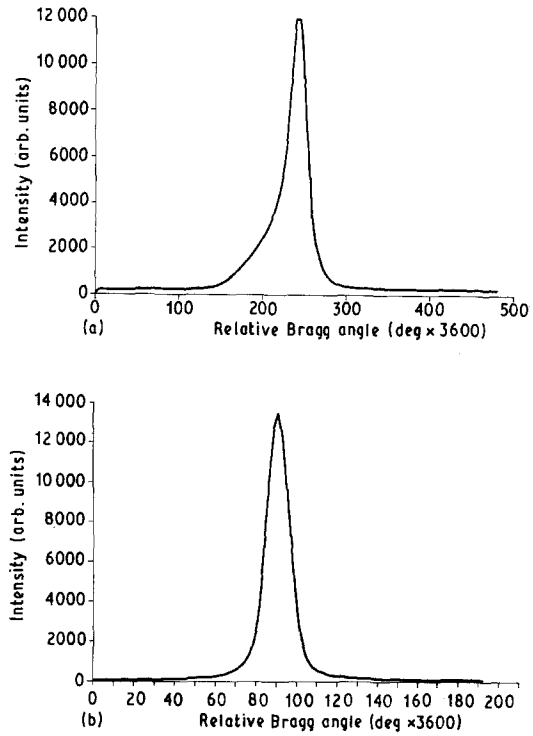

Figure 2 X-ray diffraction spectra of virgin materials: (a) early material, (b) later material.

shown in Fig. 2b being the most recent. The narrowing of the single diffraction peak in the later material indicates a significant improvement in crystal quality over that period. Diffusion of the optical waveguide results in the appearance of a second, relatively narrow, peak indicating the presence of a well defined region of different lattice constant, the Ti-diffused waveguide layer. This is clearly demonstrated in Fig. 3, which shows the corresponding diffraction spectra obtained from finished devices of the A and B types, indicating significant differences. Specifically, whereas the former shows the appearance of the waveguide region distinctly, in the type B device (the type showing no evidence of acousto-optic interaction) the surface region is considerably less well ordered, as indicated by the lack of resolution of the peaks, despite being fabricated on material of initially superior quality.

The effect of argon ion bombardment at 600 eV was investigated by subjecting a diffused waveguide to a total dose of 2.8×10^{17} ion, followed by 100 W oxygen plasma treatment for successively increasing total times up to 60 min, replicating the process used for fabrication of the type B devices. X-ray diffraction spectra were taken following each incremental oxygen plasma treatment stage; data extracted from these spectra is collected in Table II for ease of comparison. Qualitatively, argon bombardment broadens the low-angle peak associated with the waveguide region while simultaneously increasing the peak separation, i.e. the actual lattice distortion in the waveguide region increases by a factor of 20%. Subsequent oxygen plasma treatment at 100 W, while partially enhancing the resolution of the two phases, does little to restore the original condition; some reduction in the waveguide-region broadening is evident for treatment periods up

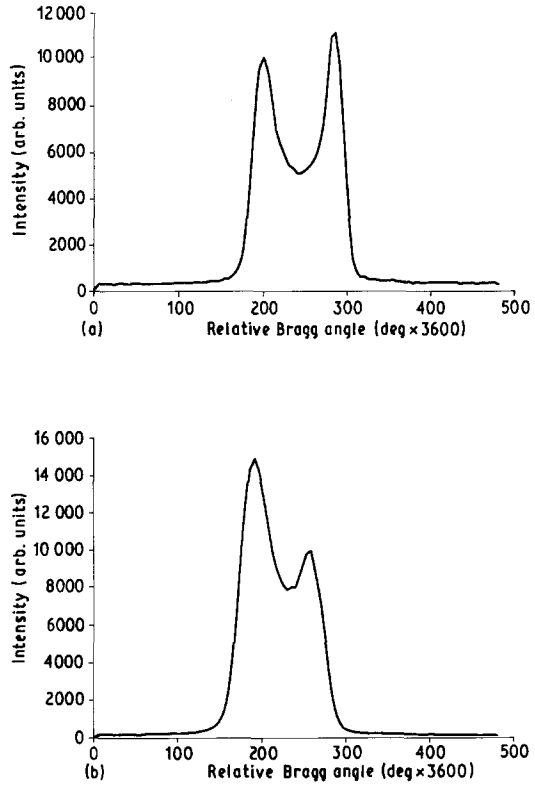

Figure 3 X-ray diffraction spectra of finished devices: (a) type A device, (b) type B device.

TABLE II Lithium niobate surface crystallography – summary of X-ray diffraction results

Sample	Peak separation	Trough amplitude	Width (Lo)	Width (Hi)
Virgin				
Old			28.5	
New			11.6	
Diffused	65.99	45	17.0	10.2
Ar^+ etched	78.23	44	19.1	10.2
Oxygen plasma ash				
15 min	78.23	41	16.3	7.8
30 min	79.93	38	15.7	7.8
45 min	82.31	39	16.9	9.5
60 min	78.23	43	18.0	11.6
Annealed 200 °C	79.93	35	14.3	7.1

to 30 min, presumably reflecting some degree of stoichiometry stabilization in this region, but longer exposure to the plasma results in further broadening.

Finally, in the light of the observations of Schreck and Dransfeld [11], Table II also shows the effect of an 8 h thermal anneal at 200 °C. Both substrate and waveguide regions show marked narrowing, indicating an overall improvement in lattice quality; the peak resolution is correspondingly enhanced, although the additional peak separation, and hence lattice distortion, consequent on the argon ion bombardment, is not removed.

3.4. Electrical properties

The influence of thermal annealing on surface resistivity is readily seen by direct electrical measurement of device structures. A newly fabricated type B transducer exhibited a d.c. resistance of 1.2 MΩ equivalent to a surface resistivity of 1.6×10^9 Ω/□. After annealing at 200 °C for 8 h, a transducer of identical geometry had an unmeasurable d.c. resistance (in excess of 33 MΩ), equivalent to a surface resistivity greater than 4.4×10^{10} Ω/□. By comparison, the device described by Schreck and Dransfeld [11] had a surface resistivity of 1.5×10^{13} Ω/□.

4. Thermal annealing of assembled acousto-optic devices

As already noted, type B devices exhibited no evidence of acousto-optic interaction, when operated under conditions under which nominally identical type A devices showed acousto-optic diffraction efficiencies in excess of 5%. Schreck and Dransfeld [11] observed that the surface of Ar^+-bombarded lithium niobate was restored to its original condition by thermal annealing at 200 °C for a period of 24 h. On the basis of confirmatory evidence obtained from the X-ray diffraction studies, a comparable annealing process was undertaken on type B devices, with the object of establishing whether this treatment would restore acousto-optic behaviour. Two fully processed device chips were subjected to a 200 °C anneal for a period of 8 h, care being taken to prevent pyroelectric damage to the 650 nm wide transducer fingers. Annealed devices were assembled on to standard carriers with strip line feeders, and were wire-bonded in the standard manner. Initial attempts at device operation were entirely successful, good visual diffraction, comparable with the best seen in previous devices, being readily observed at an optical wavelength of 633 nm; this process was found to be consistently repeatable. Fig. 4 shows the frequency dependence of acoustic wave attenuation in lithium niobate previously reported by Slobodnik *et al.* [14], together with the result obtained from the annealed type B device, the very good agreement indicating complete restoration of the surface acoustic wave properties.

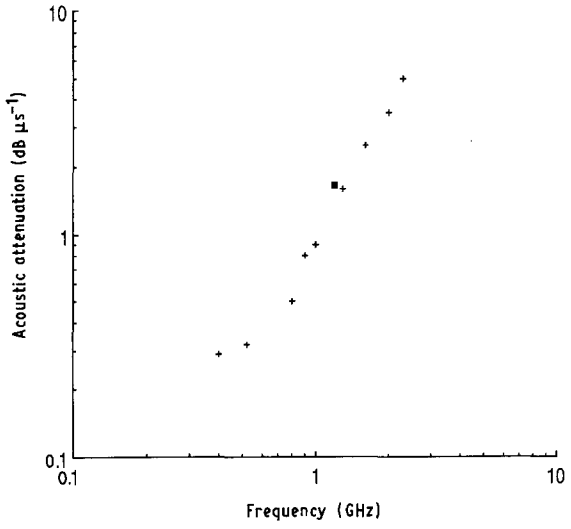

Figure 4 Frequency dependence of surface acoustic wave attenuation of lithium niobate: (+) data from Slobodnik *et al.* [14], (■) present work.

5. Conclusions

The present investigation has confirmed the significance of low-energy particle bombardment as a material damage process, particularly as it affects electrical and electro-mechanical properties, and has shown that, for certain substrates of technological interest, the effects of low-energy ion-milling and reactive ion-etching processes cannot be regarded as being limited to mere material removal, but must be viewed in the context of material modification and surface layer generation. Although great care is generally taken to prevent damage to lithium niobate surfaces under high-energy bombardment, it is apparent that similar precautions must also be taken to prevent damage under low-energy irradiation and that post-processing damage removal techniques must be developed for each material system liable to be affected.

Acknowledgements

The author wishes to thank R. M. Gibbs for device fabrication and for skilfully performing the annealing experiments, D. G. Hart for X-ray diffraction measurements and D. J. Robbins for help in performing implantation simulation calculations. The work reported here has been supported in part by the European Space Agency under ESTEC contract No. 6648/86/NL/PB(SC).

References

1. R. S. WEIS and T. K. GAYLORD, *Appl. Phys. A* **37** (1985) 191.
2. A. RAUBER, *Curr. Topics in Mater. Sci.* **1** (1978) 481.
3. I. BENNION, *Natl Electron. Rev.* **22** (1987) 57.
4. D. R. BRAMBLEY, C. J. G. KIRKBY, C. STEWART and W. J. STEWART, in Technical Digest of the International Conference on Integrated Optics and Optical Communications (IOOC '83), (Japanese Institute of Electronic and Communications Engineering, Tokyo, 1983) Paper 30B3-4, p. 256.
5. G. L. DESTEFANIS, J. P. GAILLARD, E. L. LIGEON, S. VALETTE, B. W. FARMERY, P. D. TOWNSEND and A. PEREZ, *J. Appl. Phys.* **50** (1979) 7898.
6. R. COURTHS, P. STEINER, H. HOCHST and S. HUFNER, *Appl. Phys.* **21** (1980) 345.
7. FENG XIQI and SHENG WEI, *Chinese Phys. Lett* **6** (1989) 72.
8. A. KLEKAMP, H. DONNERBERG, W. HEILAND and K. J. SNOWDON, *Surf. Sci.* **200** (1988) L465.
9. A. KLEKAMP, K. J. SNOWDON and W. HEILAND, *Radn. Eff. & Defects in Solids* **108** (1989) 241.
10. N. A. ASTAKHOVA, M. V. STREL'TSOV and Yu. V. TSVETKOVA, *Phys. Chem. Mater. Treat.* **21** (1987) 30.
11. E. SCHRECK and K. DRANSFELD, *Appl. Phys. A* **44** (1987) 265.
12. F. S. HICKERNELL, K. D. RUEHLE, S. J. JOSEPH and G. M. REESE, in Proceedings of 1985 Ultrasonics Symposium, San Francisco, October (IEEE, New York, 1985) p. 237.
13. T. R. LARSON, W. H. WEISENBERGER and W. H. LUCKE, *Appl. Phys. Lett.* **22** (1973) 617.
14. A. J. SLOBODNIK, P. H. CARR and J. BUDREAU, *J. Appl. Phys.* **41** (1970) 4380.
15. R. G. HUNSPERGER, J. A. HUTCHBY and D. E. EBERLE, Unpublished Results cited in Larson *et al.* [13].
16. Yu Ya. TOMASHPOLSKY, *Ferroelectrics* **94** (1989) 355.
17. C. STEWART, W. J. STEWART and G. E. SCRIVENER, *Elect. Lett.* **17** (1981) 971.
18. J. F. ZEIGLER, J. P. BIERSACK and U. LITTMARK, in "The Stopping and Range of Ions in Solids" (Pergamon, New York, 1985) pp. 202–63.
19. G. B. HOCKER and W. K. BURNS, *IEEE J. Quant. El.* **QE-11** (1975) 270.
20. A. J. SLOBODNIK and E. D. CONWAY, in "Microwave Acoustics Handbook", Vol. 1A, "Surface Wave Velocities" (AFCRL, Hanscom AFB, MA 01731, USA, unpublished Technical Report No. TR-73-0597, 1973).

Received 6 March
and accepted 1 July 1991